Comparative Study of Soft Template on Gunningite Synthesis for Ibuprofen Adsorption Application

Maria Ulfa* **and Windi Apriliani**

Study Program of Chemistry Education, Faculty of Teacher Training and Education, Sebelas Maret University, Jl. Ir. Sutami 36A, 57126 Surakarta, Central Java, Indonesia

* ***Corresponding author:***

email: mariaulfa@staff.uns.ac.id

Received: November 11, 2022
Accepted: February 18, 2023

DOI: 10.22146/ijc.79098

Abstract: *This study aimed to investigate the effect of soft template variations on Zinc Sulfate Hydrate (Gunningite) synthesis and the maximum adsorption capacity of ibuprofen. This study employed the soft template method and hydrothermal at 100 °C, followed by calcination at 550 °C. Here, $ZnSO_4$ heptahydrate was used as the precursor for different templates. XRD analysis exhibited that the crystal sizes of Gunningite-F127G, Gunningite-F127, Gunningite-P123G, Gunningite-P123, and Gunningite-G were 18.35; 25.33; 25.67; 27.30; and 24.24 nm with crystallinity degrees of 36.89; 42.62; 46.83; 41.27; and 40.62%, respectively. FTIR examination indicated that the five samples contained functional groups of OH stretching at 3170 cm^{-1}, Zn-O-Zn at 1637 cm^{-1}, Zn-S=O symmetric and asymmetric at 900 and 1056 cm^{-1}, and Zn-O at 521 cm^{-1}. Furthermore, SEM-EDX investigation revealed that the morphology of all Gunningite samples was inhomogeneous due to agglomeration. Besides that, the elemental compositions in the samples were dominated by Zn and O elements. The maximum adsorption capacity obtained from each sample was 221.1 mg/g (Gunningite-F127G); 226.06 mg/g (Gunningite-F127); 234.23 mg/g (Gunningite-P123G); 229.76 mg/g (Gunningite-P123); and 222.85 mg/g (Gunningite-G). Moreover, the Gunningite kinetic model of ibuprofen adsorption followed Ho and McKay's pseudo-second-order kinetic model.*

Keywords: *Gunningite; ibuprofen; P123; F127; gelatin*

■ INTRODUCTION

Pharmaceutical waste in waters derives from factory waste and the results of human body excretion. These wastes are in the form of beta blockers, non-steroidal anti-inflammatory drugs (NSAIDs), antibiotics, antiepileptic drugs, lipid regulators, and hormones [1]. One of the most commonly detected drugs in sewage treatment plants is Ibuprofen, with a concentration of 25 mg/L [2]. Ibuprofen is a type of drug that is extensively consumed in various parts of the world. For example, it has become one of the five most consumed drugs in the UK. Ibuprofen is a non-steroidal anti-inflammatory drug (NSAID), an analgesic, and an antipyretic drug used to treat rheumatism, relieve pain, and reduce fever. Ibuprofen is soluble in organic solvents but insoluble in water.

Toxicological studies have exposed different sensitivities of aquatic organisms to ibuprofen levels. In small amounts, ibuprofen can inhibit the reproductive capacity of Daphnia Magna. Ibuprofen can inhibit lotus growth at levels of 0.4 g/m^3, whereas, at 0.2 g/m^3 and 0.1 g/m^3, it can affect the estrogen production of aquatic organisms and delay the hatching of Japanese yolk eggs, respectively [3]. Ibuprofen has been revealed to disrupt aquatic ecosystems. Among others, it affects the reproduction of invertebrates and vertebrates, fungi, and the growth of bacterial species; genetic and systemic damage to some shellfish fish species; and cytogenic properties in freshwater bivalves [4].

Several techniques have been conducted to overcome this pharmaceutical waste, one of which is the adsorption method. This technique can handle various levels of pollutants. In addition, it is also more efficient, easy to operate, not affected by toxins, suitable for continuous and partial processes, and the adsorbent can

be regenerated and used repeatedly [5]. One of the potential adsorbents is Gunningite which is a stable material containing zinc sulfate and monohydrate. Studies concerning Gunningite for ibuprofen adsorption are still very rare [6-7]. Materials previously used for the adsorption of ibuprofen include material-based carbon and silica. However, the stability and affinity of these materials were lacking [1,3,8]. The affinity of carbon or silica for ibuprofen was low. It can be compared from the electronegativities of C (2.5), Si (1.8), and Zn (1.6) [9] compared to O (3.5) in the O-H group, which has different electronegativities, respectively are 1.0, 1.7 and 1.9. With a high difference in electronegativity from Gunningite when interacting with Ibuprofen, it gives the advantage of attracting many ibuprofen molecules during the adsorption process.

Gunningite has been applied as an advanced material storage in the electrical field [10-11] and is a promising adsorbent for pollutant molecules [6-7]. Many technologies have been developed in synthesizing material particles, primarily to attain nanometer-sized particles, one of which is the dissolving process using either the sol-gel, hydrothermal, solvothermal, or self-assembly methods [12]. The sol-gel method is a promising way that needs a soft template as a structure directing agent for the main element of the material through intermolecular or intramolecular interaction forces. However, it generally only involves one template type and mainly uses synthetic templates such as Pluronic P123, Pluronic F127, or CTAB. On the one hand, the issue of environmentally friendly chemistry has occupied an important position in this century to color various scopes of material synthesis, including replacing synthetic template materials with natural materials such as gelatin. Even though it is an important issue, research to observe differences in the effect of synthetic templates, natural templates, or a combination of both on materials is rarely carried out.

Types of synthetic soft templates often employed in synthesizing uniform materials include Pluronic F127 [13], Pluronic P123 [14], CTAB [15], and CTAC [16]. Pluronic F127 (MW 12500 g/mol) belongs to the biocompatible poloxamers group and is widely used in clinics for various purposes. F127 is an amphiphilic polymer consisting of two PEO chains as the hydrophilic part and one PPO Poly(Propylene Oxide) chain as the hydrophobic part. F127 can be employed as a non-ionic emulsion surfactant due to its different polarity properties. Not only F127, Pluronic P123 or poly(ethylene oxide)-poly(propylene oxide)-poly(ethylene oxide) (PEO-PPO-PEO), having a molecular weight of 5750 g/mol, is also a dominant hydrophobic copolymer. Pluronic P123 has a relatively low critical micelle concentration (CMC) in water at about 0.313 M at 20 °C [17]. It is an excellent reason to select P123 as a sensitive surfactant to direct material structure in certain pore sizes at different temperatures. However, the high cost, low sustainability, time consumption, and complicated production are the arguments for minimizing or removing synthetic surfactants. Nevertheless, this matter can be solved by replacing the synthetic template with a natural template.

One of the natural templates is gelatin (MW close to 20000 g/mol) which can be obtained from the hydrolysis of animal skin, bone, and white fibrous tissue. The gelatin sources are sustainable and have an amine group as a high-affinity part to interact with other elements with lower electronegativity. As shown in previous research, the polar and non-polar groups in gelatin are an excellent reason to use them as a natural template. Based on the description, this work was conducted on the effects of soft template variations of F127, P123, and gelatin and their combinations to obtain Gunningite. After Gunningite had been successfully synthesized, further characterization was done to determine the crystallinity, morphology, functional groups, and adsorption capacity towards Ibuprofen.

■ EXPERIMENTAL SECTION

Materials

The materials used in this study were Pluronic P123 (EO20PO70EO20) Amphiphilic Block Copolymer (MW 5790 g/mol), Pluronic F127 Poly(ethylene glycol)-*block*-poly(propylene glycol)-*block*-poly(ethylene glycol) diacrylate (MW 12,500 g/mol), gelatin (pure analysis, MW 400 KDa), ethanol, ibuprofen (2-[4-(2-methyl

propyl) phenyl]propanoic acid), $ZnSO_4 \cdot 7H_2O$, and *n*-hexane that were obtained from Sigma Aldrich and used without prior pretreatment.

Instrumentation

The characterizations of the synthesized Gunningite samples involved several instruments, including X-Ray Diffraction (XRD) XRD/MAX-2550 HB/PC (Rigaku Co., Tokyo, Japan), Scanning Electron Microscopy (SEM) (JEOL JMS-700), and Fourier Transform Infrared (FTIR) with spectra recorded with a Bruker Vertex 70 spectroscope. The SEM-EDX test was performed at a voltage of 15.0 kV with a magnification of 10,000×. Meanwhile, the FTIR analysis was done at a wavelength of 500–4000 cm^{-1}.

Procedure

Gunningite synthesis process

Ethanol (190 mL) was dropped with a flow rate of 3 mL/min into 3.6 g of F127/1.7 g of P123 with a burette at room temperature while it was stirred. The Erlenmeyer was kept from the air during the dripping process by covering it with plastic wrap. After the process was finished (± 4–5 d), 0.0346 g of 0.1% gelatin was added. Then, the mixture was stirred for 60 min. Next, 55.39 g of $ZnSO_4$ heptahydrate were added and stirred for 24 h in a closed state with plastic wrap so that no air entered. Afterward, the sample was put into a hydrothermal reactor and heated at 100 °C for 24 h. Then, the sample was left to cool. The white solid was filtered through a Buchner filter and washed with distilled water until it obtained a pH of 7. The solid was heated in an oven at 100 °C for ± 5 h. Then, it was calcined in a furnace at 550 °C for 12 h. The synthesized sample in the form of a white solid was stored in a closed, clear bottle (vial). The samples synthesized in this study were five types labeled in Table 1.

Characterization

Gunningite with various soft templates was characterized using Fourier transform infrared spectrophotometer (FTIR, Shimadzu 2100)- with a KBr pellet at a spectral resolution of 4 cm^{-1}, operated from 400–4000 cm^{-1} to analyze the functional group of the sample. Then, X-ray diffraction (XRD) (XRD-MAX-2550-Rigaku Co., Tokyo, Japan with 40 kV, 30 mA) at a range of $2\theta = 5$ to 80° was performed to observe the crystallinity of the Gunningite. Scanning electron microscope (SEM, (JEOL JMS-700) coated by Pd/Au was employed to investigate the phase structure morphology of Gunningite.

Ibuprofen adsorption process

Ibuprofen was dissolved with hexane as a solvent to obtain 100 mL of ibuprofen with an initial concentration of 100 mg/L. Then, 50 mL of ibuprofen solution was taken and put in a beaker. Next, 0.02 g of gunningite was added to the beaker containing ibuprofen while it was stirred for 50 min at room temperature and closed. Afterward, 3 mL of the sample solution was taken every 5 min and analyzed by UV-Vis spectroscopy (model U-2000, Hitachi, Japan) at 272 nm wavelength.

■ RESULTS AND DISCUSSION

XRD analysis was performed to gain information about the atomic size of crystalline and non-crystalline materials and determine the crystal structure and the orientation of the polycrystalline solid or powder sample.

Table 1. The type of samples synthesized in this study

Sample	Template		
	Pluronic F127	Pluronic P123	Gelatin
Gunningite-F127G	√	-	√
Gunningite-F127	√	-	-
Gunningite-P123G	-	√	√
Gunningite-P123	-	√	-
Gunningite-G	-	-	√

Fig. 1 presents the diffraction patterns of Gunningite with variations of soft templates. It exhibits that all samples matched the Gunningite standard (JCPDS-96-900-9374). It indicated that all Gunningite samples had been successfully synthesized with $ZnSO_4{\cdot}H_2O$ as the ideal formula. It is in line with previous research [6,18]. Furthermore, the peaks of the diffractogram could be exploited to estimate the crystal size using the Debye-Scherrer equation. The results demonstrated that the crystal sizes of Gunningite-F127G, Gunningite-F127, Gunningite-P123G, Gunningite-P123, and Gunningite-G were 18.35; 25.33; 25.67; 27.30; and 24.24 nm with the crystallinity degrees of 36.89; 42.62; 46.83; 41.27; and 40.62%, respectively. The largest crystal size was achieved by Gunningite-P123. It was due to the high hydrophobic part compared to the other soft templates, which attains the large crystal size by intermolecular forces. An interesting result came from the combination of P123 and the gelatin soft template (Gunningite-P123G), which obtained the highest crystallinity at 46%. This is due to the synergy of the amine group from gelatin and the hydrophilic-hydrophobic parts or P123 to attain gunningite crystallinity degree during high-temperature treatment.

The effect of the different soft templates was also confirmed by SEM to determine the synthesized compounds' morphology, crystal growth distribution, and physical changes in the preparation conditions. Observations were made with a magnification of 10,000× and completed by EDX measurement to investigate elemental compositions.

Fig. 2 displays that the five samples had inhomogeneous particle shapes due to agglomeration. The morphology of the gunningite from P123, F127, gelatin, and their combination was a disordered hexagonal flake, disordered cuboid, disordered sphere, and the combination of sphere and flake. All Gunningite

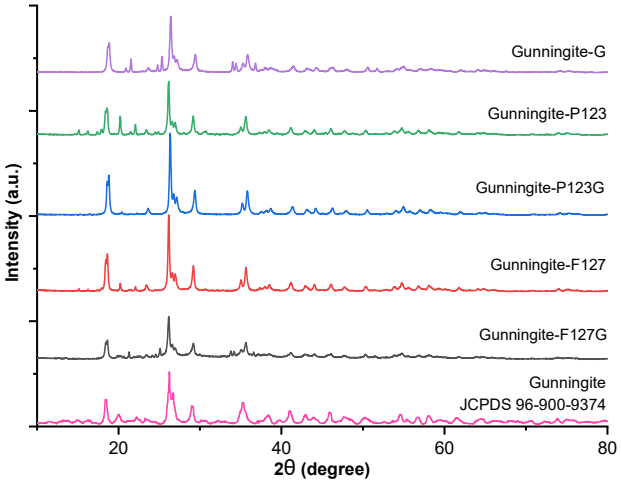

Fig 1. Diffraction patterns of Gunningite with variations of soft templates

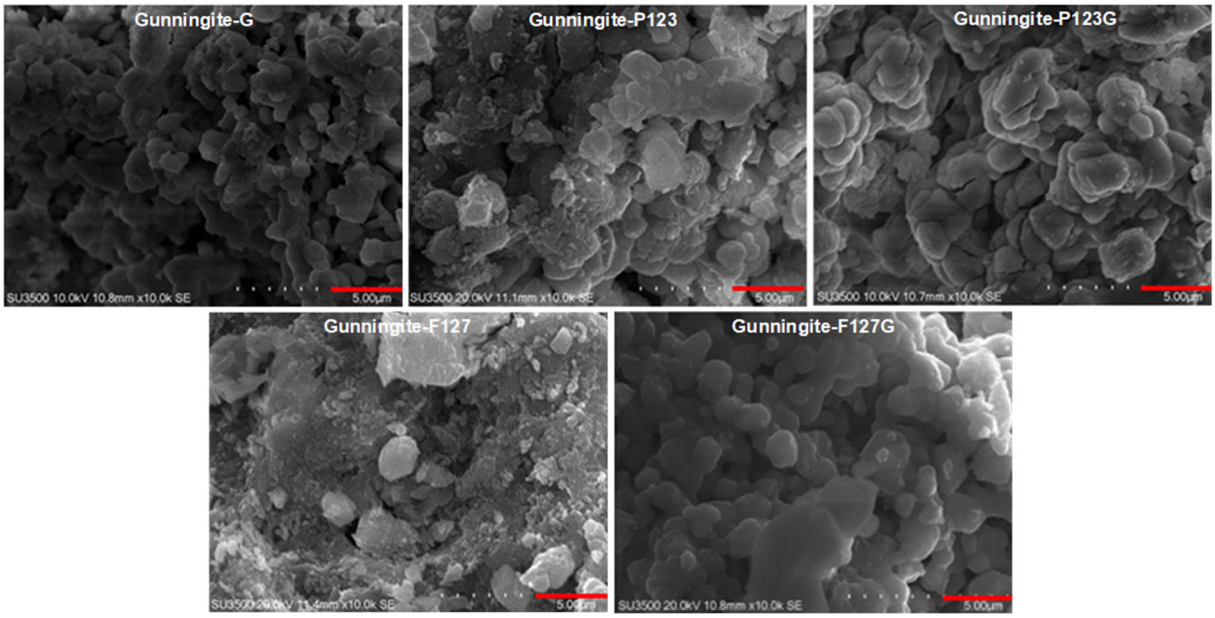

Fig 2. SEM images of Gunningite using the different templates

samples were agglomerated to obtain stable particle size and maintain the particle size distribution by direct hydrophobic-hydrophilic parts to interact with the precursor of Gunningite.

Fig. 3 shows the histogram of the particle size distribution from the SEM analysis. It shows that Gunningite reached the most uniform particle size distribution at P123 at 0.67992 μm (Fig. 3(a)). It then decreased to 0.65442 μm when combined with gelatin (Fig. 3(b)). However, the combination of F127-Gelatin showed the largest particle distribution size at 0.76316 μm (Fig. 3(e)). It was due to the interaction between the amine group in gelatin and the carbon chain of F127. These phenomena conclude that the domination of the hydrophobic part (PPO on P123) from the synthetic template and the amine group from the natural template decreases the particle size distribution due to the repulsive force between them. On the other hand, the domination of the hydrophilic part from the synthetic template (PEO in F127) with the hydrophobic part from

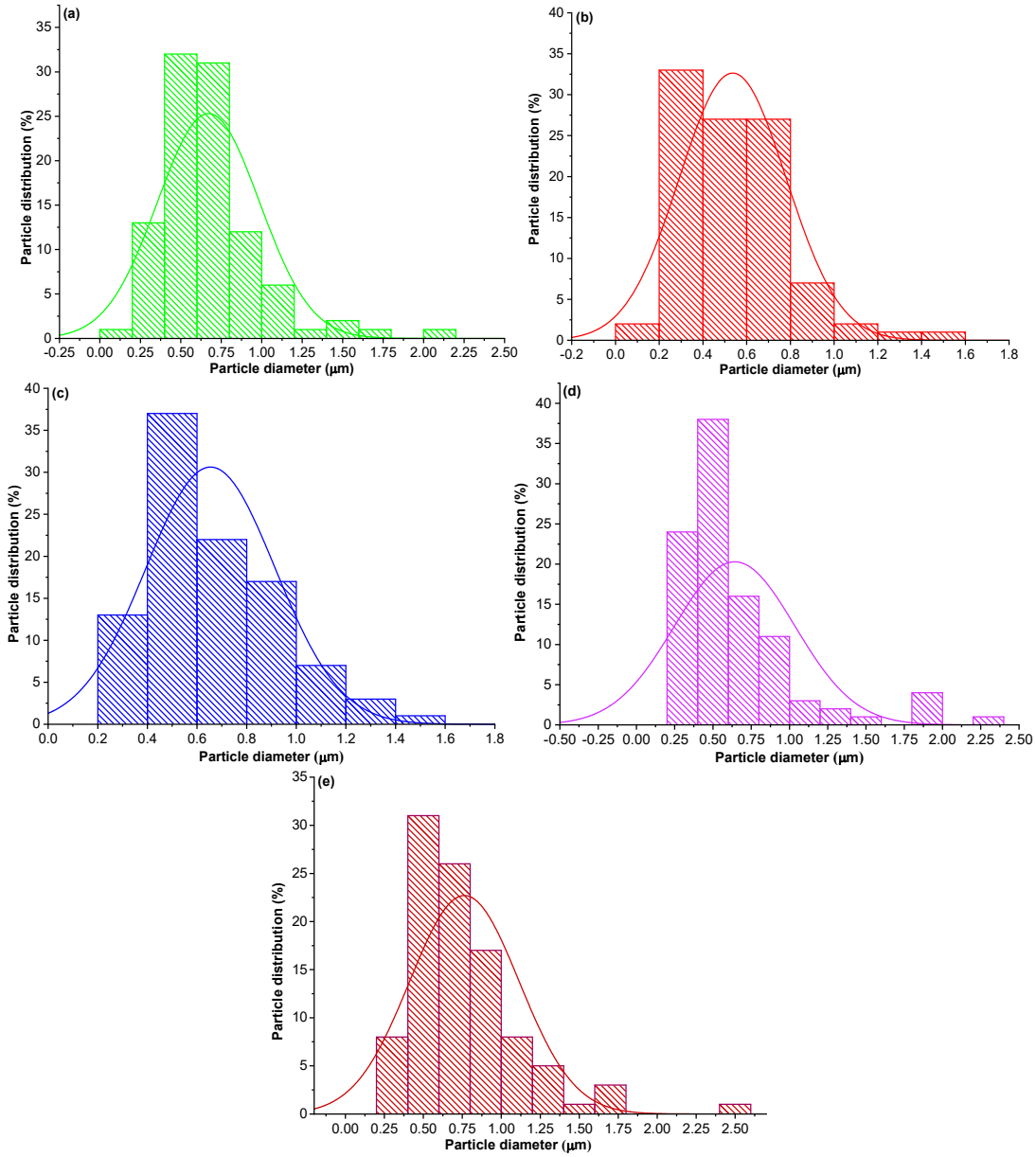

Fig 3. Particle size distribution of Gunningite using the templates of (a) Gelatin; (b) P123; (c) P123-Gelatin; (d) F127; and (e) F127-Gelatin

the natural template (amine group) increases the particle size distribution due to the high attraction between them due to intermolecular interaction, which is in line with previous studies [5,13,19-21].

Table 2 presents the EDX results of all Gunningite samples containing Zn (67–75%), S (8.5–10%), and O (13.4–16.4%), implying the stable composition to obtain the formula of $ZnSO_4 \cdot 1H_2O$. The results revealed that gunningite synthesized with only P123 produced an impurity of carbon (Fig. 4(a)). It is because there is no high affinity in the functional group (such as the amine group from gelatin that pulls carbon out of the molecule during decomposition). However, Gunningite with only gelatin produced sodium as the impurity from gelatin extraction by NaOH (Fig. 4(b)). The good news was all Gunningite with only F127 (Fig. 4(d)), F127-gelatin (Fig. 4(e)), and P123-gelatin (Fig. 4(c)) exhibited high purities where P123-gelatin and F127 reached the highest composition of Zn. This is due to the synergy of the hydrophilic part and amine groups to maintain Gunningite's structure stability during decomposition.

Fig. 5 shows that the strong and broad absorption at about 3170 cm^{-1} was the stretching vibration of the hydroxyl group of the water molecule originating from the monohydrate molecule in gunningite. Another air molecule could be found at the absorption of 1637 cm^{-1} as Zn-O-Zn bending vibrations. The strain vibrations at about 900 cm^{-1} were due to the presence of sulfate groups whose vibrations were symmetrical and asymmetrical S=O at 1056 cm^{-1}. This peak confirmed the presence of a S=O group on the sulfate group that occurred from the electrostatic interaction between hydrogen and zinc ions in the form of S=O-H-O-Zn. In contrast, the presence of Zn elements is indicated by the peak at 521.81 cm^{-1} as the Zn-O form. All of these results were in line with previous studies [6-7,10,18,22].

Table 2. EDX results of all Gunningite samples using various soft templates

Template	% W			
	Zn	S	O	C
Gelatin	71.2	10.1	16.4	-
P123	67.2	8.9	16.4	7.6
P123-Gelatin	76.9	8.5	14.6	-
F127	76.9	8.9	14.2	-
F127-Gelatin	75.9	8.9	13.4	-

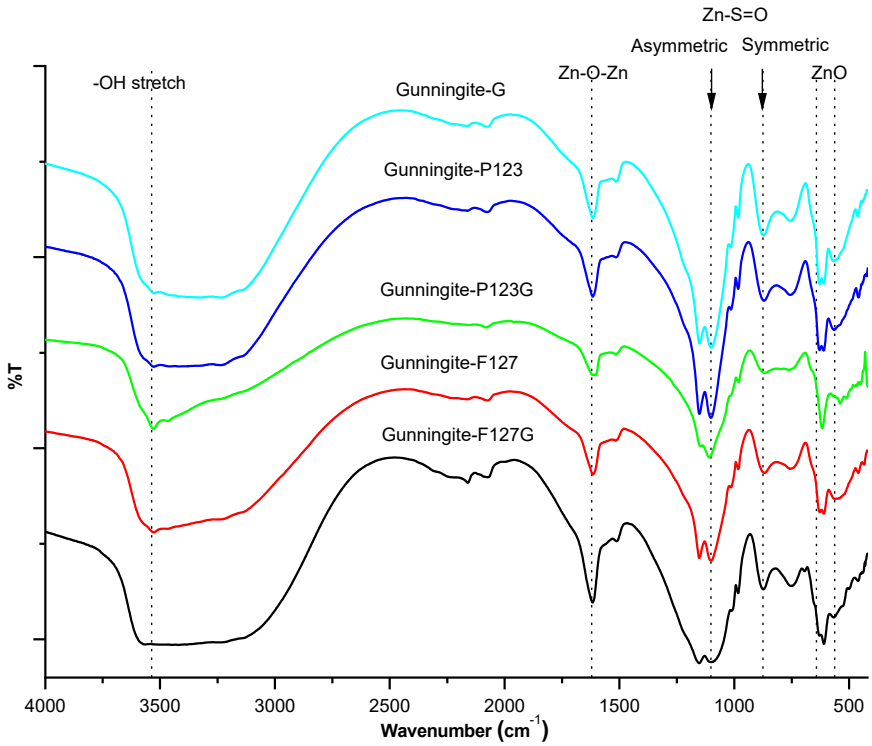

Fig 5. FTIR spectra of all Gunningite from different template

Fig. 6 exhibits the maximum adsorption capacity of Gunningite on ibuprofen adsorption. Additionally, Table 1 presents the percentage of ibuprofen removal by Gunningite using templates of F127G, F127, P123G, P123, and G which was 86.9; 84.3; 93.8; 84.2; and 84.3%, respectively. Thus, the highest adsorption was found in the Gunningite-P123G sample. It was due to the highest Zn component among all samples. The Zn element, as the adsorption center, interacts with the OH group of ibuprofen through electrostatic forces. The highest elemental composition of Zn in the Guningite-P123G sample was also observed from FTIR in the form of the sharpest/regular absorption compared to other samples, so the adsorption power of ibuprofen became greater as well.

Besides the amount of Zn in Gunningite, the low sulfur component indicated high adsorption removal performance. It was because Gunningite as the adsorbent and ibuprofen as the adsorbate also affected the adsorption capacity. The Gunningite compound acts as an adsorbent, and ibuprofen acts as an adsorbate interacting competitively between Zn-O-ibuprofen and S-O-ibuprofen. If the amount of sulfur is low, the interaction will occur on the hydroxyl group of ibuprofen with metal ions Zn^{2+}, allowing the formation of a stable covalent coordination complex. Fig. 7 demonstrates the adsorption scheme of ibuprofen onto Gunningite.

The adsorption kinetics models performed in this study were pseudo-first-order and pseudo-second-order. The models were used to process data on the ibuprofen adsorption by Gunningite, determine the adsorption variables involved, and select the adsorption mechanism that occurs. The adsorption kinetics model can also predict the speed of adsorbate transferring from solution to adsorbent [23-24]. Table 3 presents the calculation results of the adsorption kinetics models of gunningite using pseudo-first-order and pseudo-second-order.

Fig. 8(a-b) presents the kinetic of gunningite with different templates by pseudo-first-order and pseudo-second-order models. The graphs reveal linear equations obtained by each sample. Based on Table 3 and Fig. 8(a),

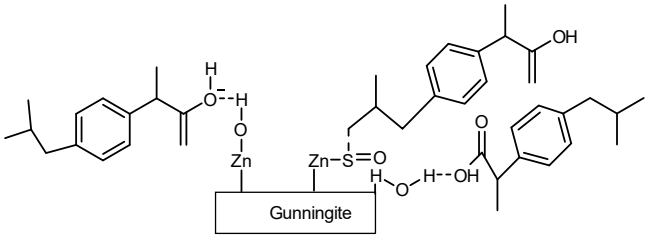

Fig 7. Adsorption scheme of ibuprofen onto Gunningite

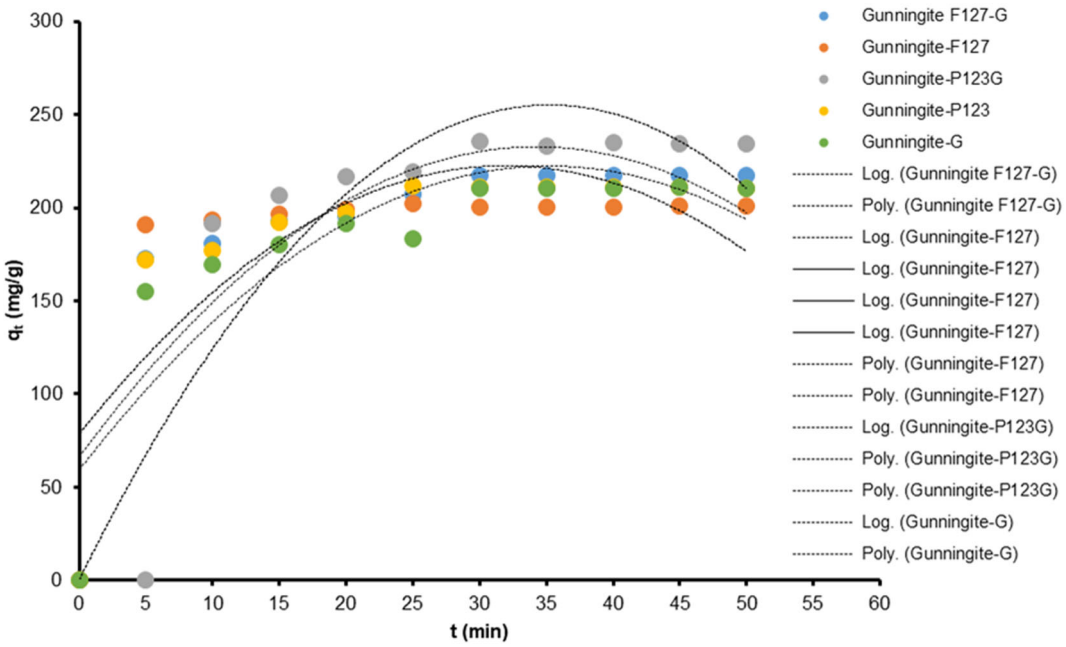

Fig 6. Adsorption performance of all sample of Gunningite

Table 3. Adsorption kinetics models of Gunningite using pseudo-first and pseudo-second-order

	Gunningite with various soft templates				
	F127-G	F127	F123-G	P123	G
Pseudo-first-order model: $\ln(q_e - q_t) = \ln q_e - k_1 t$					
k_1	0.0246	0.0214	0.1092	0.0205	0.0025
q_{cal}	0.1143	0.6149	3.6751	0.852	1.283
R^2	0.0748	0.0687	0.779	0.0905	0.0009
Pseudo-second-order model: $\left(\frac{t}{q_t} - \frac{1}{k_2 q_e q_e}\right) = kt$					
k_2	0.0047	0.0046	0.0048	0.0044	0.0045
q_{cal}	0.0024	0.0005	0.0029	0.0009	0.0014
R^2	0.9951	0.9949	0.9936	0.9996	0.9981
%Rem	86.9	84.3	93.8	84.2	80.3

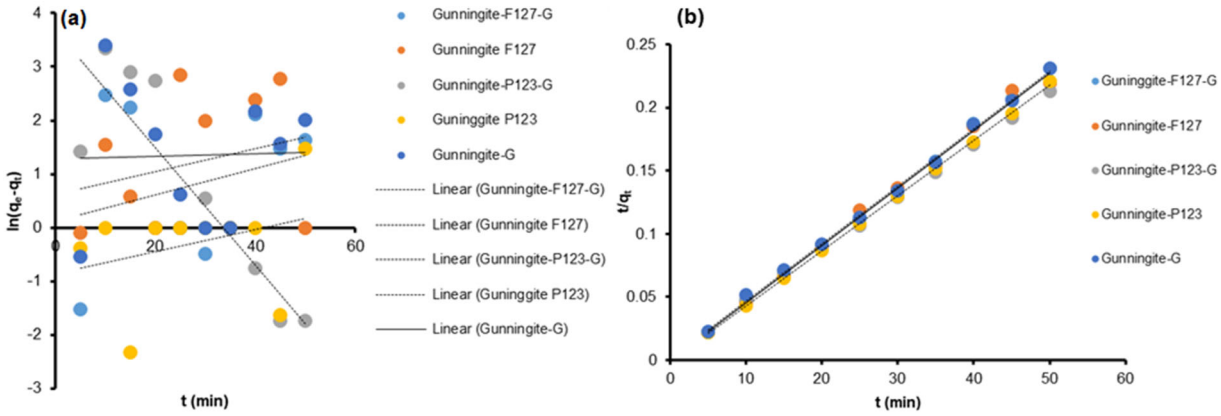

Fig 8. Kinetic of Gunningite using different templates by (a) Pseudo-first-order and (b) Pseudo-second-order model

Gunningite-F127G possessed an equation of y = 0.0246x + 0.1143 with R^2 = 0.0748. For the Gunningite-F127 sample, it was y = 0.0214x + 0.6149 with R^2 = 0.0687. Gunningite-P123 sample had an equation of y = -0.1092x + 3.6751 with R^2 = 0.779. The Gunningite-P123G sample exhibited y = 0.0205x – 0.8522 with R^2 = 0.0905. Meanwhile, the Gunningite-G sample demonstrated an equation of y = 0.0025x + 1.283 with R^2 = 0.0009. A good linear graph is a graph that has an R^2 value close to or equal to 1. Of the five samples, four samples had R^2 values that were far from 1, and only the Gunningite-P123G sample was close to 1. Besides the R^2 of the graphic equation, the suitability of the adsorption kinetics model with the ibuprofen adsorption by Gunningite could also be seen from the q_e value (adsorption capacity). With this kinetic model, the q_e values attained differed from the q_e values of the experimental results. This indicated that Lagergren's pseudo-first-order adsorption kinetics model was not suitable for the adsorption experiment of ibuprofen by gunningite. Next, the calculation was based on Ho and McKay's pseudo-second-order of adsorption kinetics model.

Based on Table 2 and Fig. 8(b), the linear equation for the Gunningite-F127G sample was y = 0.0046x – 0.0005 with R^2 = 0.999. The Gunningite-F127 sample had a linear equation of y = 0.0046x – 0.0005 with R^2 = 0.9949. Gunningite-P123G exhibited a linear equation of y = 0.0042x + 0.0047 with R^2 = 0.9988. Gunningite-P123 revealed y = 0.0044x – 0.0009 with R^2 = 0.9996. Gunningite-G presented y = 0.0045x + 0.0014 with R^2 = 0.9981. The data showed that the linearity of each graph was appropriate, as indicated by their R^2 values that were close to 1. In addition, the q_e values (adsorption capacity) based on this kinetic model were close to the q_e value of

the experimental results. This indicated that Ho and McKay's pseudo-second-order adsorption kinetics model was more suitable for the ibuprofen adsorption experiment by Gunningite. This was supported by the previous research [1-3,25-26] which demonstrated that the adsorption of ibuprofen with the pseudo-second-order adsorption kinetics model presented the best results compared to several other adsorption kinetics models, with the R^2 value on the graph ranging from 0.95–0.99 for all samples and the q_e was close to the experimental q_e value.

CONCLUSION

Gunningite nanoparticles have been successfully synthesized through the soft template method, hydrothermal at 100 °C, and calcination at 550 °C using $ZnSO_4$ heptahydrate as the precursor and various templates of F127, P123, and gelatin. The XRD results showed that the crystal sizes of the Gunningite in the template variations of Gunningite-F127G, Gunningite-F127, Gunningite-P123G, Gunningite-P123, and Gunningite-G were 18.35; 25.33; 25.67; 27.30; and 24.24 nm, respectively, while the crystallinity degrees were 36.89; 42.62; 46.83; 41.27; and 40.62%, respectively. The FTIR results exposed that the functional groups in gunningite were OH stretching, Zn-O-Zn, and gunningite. The SEM-EDX results demonstrated that the morphology of gunningite is inhomogeneous due to agglomeration, and the Zn and O elements dominated composition elements in the samples. The maximum adsorption capacity values of gunningite to adsorb ibuprofen on various templates of Gunningite-F127G, Gunningite-F127, Gunningite-P123G, Gunningite-P123, and Gunningite-G were 221.1; 226.06; 234.23; 229.76; and 222.85 mg/g, respectively. The gunningite kinetic model of ibuprofen adsorption followed Ho and McKay's pseudo-second-order kinetic model.

ACKNOWLEDGMENTS

The author would like to express special thanks to the Ministry of Research and Technology National Research and Innovation Agency (DIKTI) Indonesia for the funding grants on Fundamental research under No. 469.1/UN27.22/PT01.03/2022/2022 for Maria Ulfa from Sebelas Maret University.

AUTHOR CONTRIBUTIONS

Maria Ulfa, conceived and designed the experiments, concept, and method; analyzed, investigated, and interpreted the data analysis; contributed reagents and materials; wrote, revised, edited, reviewed, and supervised the manuscript. Windi Apriliani conducted the analysis tools or data, wrote the raw paper, and conducted the experiment and formal calculations. All authors agreed to the final version of this manuscript.

REFERENCES

[1] Manzano, J.S., Singappuli-Arachchige, D., Parikh, B.L., and Slowing, I.I., 2018, Fine-tuning the release of molecular guests from mesoporous silicas by controlling the orientation and mobility of surface phenyl substituents, *Chem. Eng. J.*, 340, 73–80.

[2] Das, S.K., Kahali, N., Bose, A., and Khanam, J., 2018, Physicochemical characterization and *in vitro* dissolution performance of ibuprofen-Captisol® (sulfobutylether sodium salt of β-CD) inclusion complexes, *J. Mol. Liq.*, 261, 239–249.

[3] Wang, X., Liu, P., and Tian, Y., 2011, Preparation and drug release behavior of temperature-responsive mesoporous carbons, *J. Solid State Chem.*, 184 (6), 1571–1575.

[4] Ulfa, M., Prasetyoko, D., Mahadi, A.H., and Bahruji, H., 2020, Size tunable mesoporous carbon microspheres using Pluronic F127 and gelatin as co-template for removal of ibuprofen, *Sci. Total Environ.*, 711, 135066.

[5] Bouzidi, M., Sellaoui, L., Mohamed, M., Franco, D.S.P., Erto, A., and Badawi, M., 2023, A comprehensive study on paracetamol and ibuprofen adsorption onto biomass-derived activated carbon through experimental and theoretical assessments, *J. Mol. Liq.*, *376*, 121457.

[6] Ulfa, M., Ari, M., and Ali, P., 2022, Influence of calcination temperatures on gunningite-based gelatin template and its application as ibuprofen adsorption, *Indones. J. Chem.*, 22 (6), 1684–1692.

[7] Prasetyoko, D., Sholeha, N.A., Subagyo, R., Ulfa, M., Bahruji, H., Holilah, H., Pradipta, M.F., and Jalil, A.A., 2023, Mesoporous ZnO nanoparticles using gelatin — Pluronic F127 as a double colloidal system for methylene blue photodegradation, *Korean J. Chem. Eng.*, 40 (1), 112–123.

[8] Guedidi, H., Reinert, L., Soneda, Y., Bellakhal, N., and Duclaux, L., 2017, Adsorption of ibuprofen from aqueous solution on chemically surface-modified activated carbon cloths, *Arabian J. Chem.*, 10 (2), S3584–S3594.

[9] Babikier, M., Wang, D., Wang, J., Li, Q., Sun, J., Yan, Y., Yu, Q., and Jiao, S., 2014, Fabrication and properties of sulfur (S)-doped ZnO nanorods, *J. Mater. Sci.: Mater. Electron.*, 25 (1), 157–162.

[10] Ducher, M., Blanchard, M., and Balan, E., 2018, Equilibrium isotopic fractionation between aqueous Zn and minerals from first-principles calculations, *Chem. Geol.*, 483, 342–350.

[11] Tilak, S., and Suresh Kumar, H.M., 2020, Optical, thermal, mechanical, dielectric and magnetic properties of zinc sulphate doped L-ascorbic acid NLO crystal, *Mater. Today: Proc.*, 27, 503–508.

[12] Karakiliç, P., Toyoda, R., Kapteijn, F., Nijmeijer, A., and Winnubst, L., 2019, From amorphous to crystalline: Transformation of silica membranes into silicalite-1 (MFI) zeolite layers, *Microporous Mesoporous Mater.*, 276, 52–61.

[13] Yan, Y., Wei, J., Zhang, F., Meng, Y., Tu, B., and Zhao, D., 2008, The pore structure evolution and stability of mesoporous carbon FDU-15 under CO_2, O_2 or water vapor atmospheres, *Microporous Mesoporous Mater.*, 113 (1-3), 305–314.

[14] Liu, T., Lai, D., Feng, X., Zhu, H., and Chen, J., 2013, Synthesis and characterization of a novel mesoporous bioactive glass/hydroxyapatite nanocomposite, *Mater. Lett.*, 92, 444–447.

[15] Ulfa, M., Masykur, A., Nofitasari, A.F., Sholeha, N.A., Suprapto, S., Bahruji, H., and Prasetyoko, D., 2022, Controlling the size and porosity of sodalite nanoparticles from Indonesian kaolin for Pb^{2+} removal, *Materials*, 15 (8), 2745.

[16] Nagamine, S., Kurumada, K., Tanigaki, M., and Endo, A., 2001, Effects of catalytic acid and templating surfactant concentrations on mesostructure of submillimeter-thick mesoporous silica by solvent evaporation synthesis, *Microporous Mesoporous Mater.*, 49 (1-3), 57–64.

[17] He, Z., and Alexandridis, P., 2018, Micellization thermodynamics of Pluronic P123 ($EO_{20}PO_{70}EO_{20}$) amphiphilic block copolymer in aqueous ethylammonium nitrate (EAN) solutions, *Polymer*, 10 (1), 32.

[18] Buzatu, A., Dill, H.G., Buzgar, N., Damian, G., Maftei, A.E., and Apopei, A.I., 2016, Efflorescent sulfates from Baia Sprie mining area (Romania) — Acid mine, *Sci. Total Environ.*, 542, 629–641.

[19] Yang, J., Zhai, Y., Deng, Y., Gu, D., Li, Q., Wu, Q., Huang, Y., Tu, B., and Zhao, D., 2010, Direct triblock-copolymer-templating synthesis of ordered nitrogen-containing mesoporous polymers, *J. Colloid Interface Sci.*, 342 (2), 579–585.

[20] Li, S., Jiang, M., Shi, X., Liu, Z., and Zhou, G., 2017, P123 assisted morphology-engineered and hierarchical TiO_2 microspheres for enhanced photocatalytic activity, *J. Porous Mater.*, 24 (6), 1425–1436.

[21] Shi, F., Liu, J.X., Huang, X., Yu, L., Liu, S.H., Feng, X., Wang, X.K., Shao, G.L., Hu, S.C., Yang, B., and Fan, C.Y., 2015, Hydrothermal synthesis of mesoporous WO_3-TiO_2 powders with enhanced photocatalytic activity, *Adv. Powder Technol.*, 26 (5), 1435–1441.

[22] Wang, X., Wan, Y., Hu, W., Chou, I.M., Cao, J., Wang, X., Wang, M., and Li, Z., 2016, *In situ* observations of liquid–liquid phase separation in aqueous $ZnSO_4$ solutions at temperatures up to 400 °C: Implications for Zn^{2+}–SO_4^{2-} association and evolution of submarine hydrothermal fluids, *Geochim. Cosmochim. Acta*, 181, 126–143.

[23] Ho, Y.S., and McKay, G., 1999, Pseudo-second order model for sorption processes, *Process Biochem.*, 34 (5), 451–465.

[24] Ho, Y.S., 2004, Citation review of Lagergren kinetic

rate equation on adsorption reactions, *Scientometrics*, 59 (1), 171–177.

[25] Ulfa, M., Sari, A.Y., and Prasetyoko, D., 2018, Synthesis of unique natural silica (UNS) material via dual co-templating method using starch of waste rice-gelatin composite and their performance in drug delivery system, *AIP Conf. Proc.*, 2049, 020003.

[26] Lei, X., Huang, L., Liu, K., Ouyang, L., Shuai, Q., and Hu, S., 2021, Facile one-pot synthesis of hierarchical *N*-doped porous carbon for efficient ibuprofen removal, *J. Colloid Interface Sci.*, 604, 823–831.